Wider paleogeographical distribution of Bothremydid turtles in northern South America during the Paleocene–Eocene

EDWIN-ALBERTO CADENA[1,2,3]
BYRON BENÍTEZ[4]
FRANCISCO EMMANUEL APEN[5,6]

JAMES LEAHEY CROWLEY[7]
JOHN COTTLE[5]
CARLOS JARAMILLO[2]

1. Grupo de Paleontología Neotropical Tradicional y Molecular (PaleoNeo), Facultad de Ciencias Naturales, Universidad del Rosario. Quinta Mutis, Cra 24 63C-69, 111311, Bogotá, Colombia.
2. Smithsonian Tropical Research Institute, CTPA, Balboa. Ancón, 0843-03092, Panama City, Panama.
3. Field Museum of Natural History (FMNH). 1400 S Lake Shore Dr, Chicago, IL 60605, United States of America.
4. Museo de los Andes de Socha (MAS). Calle 2 N° 7-49, 151640, Socha, Departamento de Boyacá, Colombia.
5. Department of Earth Science, University of California Santa Barbara (UCSB). Lagoon Rd, Santa Barbara, CA 93106, United States of America.
6. Department of Geosciences, Princeton University. Guyot Hall, Princeton, NJ 08544, United States of America.
7. Isotope Geology Laboratory, Boise State University. 1295 W University Dr, Boise, ID 83725, United States of America.

Pe/APA | **Publicación Electrónica**
ASOCIACIÓN PALEONTOLÓGICA ARGENTINA
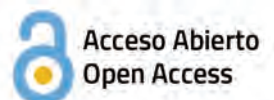
WIDER PALEOGEOGRAPHICAL DISTRIBUTION OF BOTHREMYDID TURTLES IN NORTHERN SOUTH AMERICA DURING THE PALEOCENE–EOCENE

EDWIN-ALBERTO CADENA[1,2,3], BYRON BENÍTEZ[4], FRANCISCO EMMANUEL APEN[5,6], JAMES LEAHEY CROWLEY[7], JOHN COTTLE[5], AND CARLOS JARAMILLO[2]

[1]Grupo de Paleontología Neotropical Tradicional y Molecular (PaleoNeo), Facultad de Ciencias Naturales, Universidad del Rosario. Quinta Mutis, Cra 24 63C-69, 111311, Bogotá, Colombia. *edwin.cadena@urosario.edu.co*

[2]Smithsonian Tropical Research Institute, CTPA, Balboa. Ancón, 0843-03092, Panama City, Panama. *jaramilloc@si.edu*

[3]Field Museum of Natural History (FMNH). 1400 S Lake Shore Dr, Chicago, IL 60605, United States of America.

[4]Museo de los Andes de Socha (MAS). Calle 2 N° 7-49, 151640, Socha, Departamento de Boyacá, Colombia. *byronbeniteze@yahoo.com*

[5]Department of Earth Science, University of California Santa Barbara (UCSB). Lagoon Rd, Santa Barbara, CA 93106, United States of America. *fa8816@princeton.edu*; *cottle@geol.ucsb.edu*

[6]Department of Geosciences, Princeton University. Guyot Hall, Princeton, NJ 08544, United States of America.

[7]Isotope Geology Laboratory, Boise State University. 1295 W University Dr, Boise, ID 83725, United States of America. *jimcrowley@boisestate.edu*

EAC: https://orcid.org/0000-0003-3038-567X; **CJ:** https://orcid.org/0000-0002-2616-5079; **FEA:** https://orcid.org/0000-0002-1209-3844; **JC:** https://orcid.org/0000-0002-3966-6315; **JLC:** https://orcid.org/0000-0001-5069-0773

Abstract. Bothremydidae was one of the most diverse and widespread group of side-necked turtles (pleurodirans) during the Cretaceous and part of the Paleogene. In South America, the Paleogene record of bothremydids is restricted to *Puentemys mushaisaensis* from the middle–late Paleocene Cerrejón Formation of Colombia, *Inaechelys pernambucensis* from the Paleocene of Brazil, and *Motelomama olssoni* from the early Eocene of Perú. Here, we describe two shells of *P. mushaisaensis* and several other isolated bones conferred to this taxon from the upper Paleocene and lower Eocene Arcillolitas de Socha Formation found in the Socha Region, Boyacá Department of Colombia. U-Pb dating of detrital zircon from two levels from this formation indicates maximum depositional ages of 56.83±0.04 Ma and 57.2±0.5 Ma for the *areniscas guía* interval of the formation. The new occurrence of *P. mushaisaensis* in the Socha region, at least 500 km south from Cerrejón, indicates a wider biogeographical distribution of northern South America Paleocene herpetofauna, possibly helped by low topography and ecosystems connectivity via a faunistic corridor.

Key words. Testudines. Colombia. Paleobiogeography. Bothremydidae. Arcillolitas de Socha Formation.

Resumen. DISTRIBUCIÓN PALEOBIOGEOGRÁFICA MÁS AMPLIA DE TORTUGAS BOTREMIDIDAS EN EL NORTE DE SUR AMÉRICA DURANTE EL PALEOCENO–EOCENO. Bothremydidae fue uno de los grupos de tortugas de cuello lateral (pleurodiras) más diversos y extendidos durante el Cretácico y parte del Paleógeno. En América del Sur, el registro Paleógeno de bothremididos se limita a *Puentemys mushaisaensis* de la Formación Cerrejón del Paleoceno medio–tardío en Colombia, *Inaechelys pernambucensis* del Paleoceno de Brasil, y *Motelomama olssoni* del Eoceno temprano en Perú. Aquí, describimos dos caparazones de *P. mushaisaensis* y varios huesos aislados atribuidos a este taxón de la Formación Arcillolitas de Socha del Paleoceno superior y Eoceno inferior, ubicada en la Región de Socha, Departamento de Boyacá en Colombia. La datación U-Pb de circones detríticos de dos niveles de esta formación indica edades máximas de deposición de 56.83±0.04 Ma y 57.2±0.5 Ma para el intervalo de areniscas guía de la formación. La nueva presencia de *P. mushaisaensis* en la región de Socha, al menos 500 km al sur de Cerrejón, indica una distribución biogeográfica más amplia de la herpetofauna del Paleoceno en el norte de América del Sur, posiblemente facilitada por una topografía baja y la conectividad de ecosistemas a través de un corredor faunístico.

Palabras clave. Testudines. Colombia. Paleobiogeografía. Bothremydidae. Formación Arcillolitas de Socha.

Bothremydid turtles (Bothremydidae) were a diverse clade that inhabited fluvial, deltaic, and coastal environments in South and North America, Africa, India, Madagascar, the Middle East, and Europe spanning from the Early Cretaceous (late Albian) to the Paleogene (Ypresian) (Lapparent de Broin,

2000; Gaffney *et al.*, 2006; Pérez-García, 2016; Lapparent de Broin *et al.*, 2021, and references therein).

The Paleogene fossil record of South American bothremydids is represented by three taxa: *Puentemys mushaisaensis* Cadena *et al.* (2012), belonging to the

Bothremydini tribe, from the Paleocene Cerrejón Formation of Colombia, *Inaechelys pernambucensis* from the Paleocene (Danian) Maria Farinha Formation of Brazil (De Araújo-Carvalho *et al.*, 2016), and *Motelomama* ('*Podocnemis*', '*Taphrosphys*') *olssoni*, belonging to Taphrosphyini tribe, from the Eocene of Perú (Schmidt, 1931; Gaffney *et al.*, 2006; Pérez-García, 2018a).

Recently, we discovered several fossil-rich sites in the Socha town region, Boyacá Department, Eastern Andes of Colombia (Fig. 1.1). These sites have proven to have an abundant record of turtles, crocodiles, snakes, and fishes from the middle to upper Paleocene Arcillolitas de Socha Formation (Velandia-Angarita *et al.*, 2023). In this study, we describe the fossil turtles from the Arcillolitas de Socha Formation and discuss their paleobiogeographical implications. We also present the first radiometric ages for the Arcillolitas de Socha Formation. These ages are key for placing the fossils of this formation within a regional and
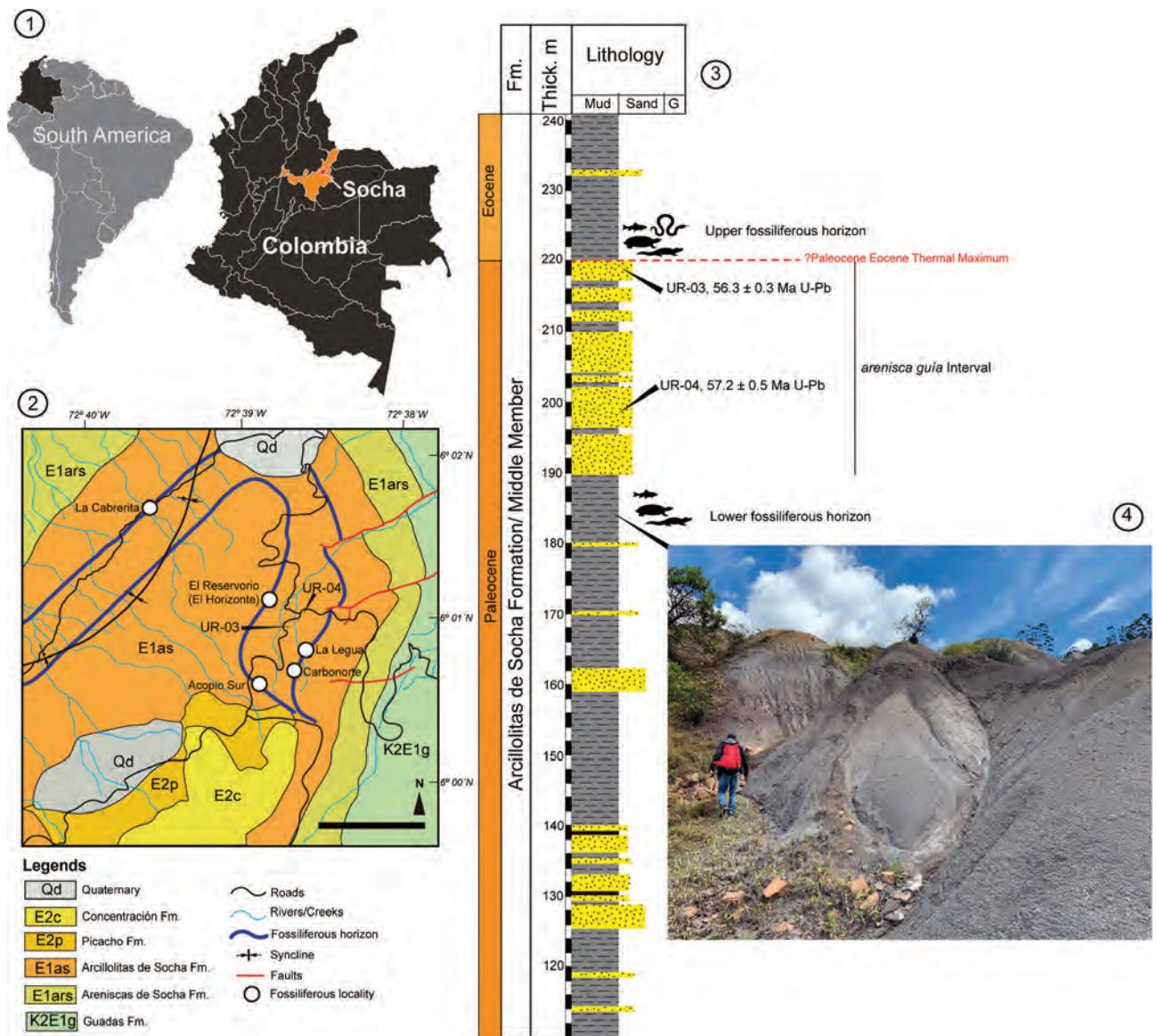
Figure 1. Geographical and geological context of Socha region. **1,** Maps of South America and Colombia indicating the location of Socha; **2,** geologic map of the Socha region where the fossils described herein come from, modified and redraw from Velandia-Angarita *et al.* (2023); **3,** stratigraphic column for the Arcillolitas de Socha Formation redraw from Velandia-Angarita *et al.* (2023), including the two fossiliferous horizons and from where the rock samples for radiometric dating were taken; **4,** photograph of the outcrop of La Cabrerita locality. Scale in 2= 1 km.

global chronological context and for inferring the potential paleoclimatic conditions under which they lived.

MATERIALS AND METHODS

Fossils. We have collected at least 58 fossil specimens over the course of a decade, which include nearly complete shells and isolated bones. In the case of isolated bones, in order to establish how many of these specimens represent single individuals, we considered size and uniqueness of the bone in the carapace. For instance, there is only one nuchal bone in the shell, which only can correspond to a single individual. Some uncertainty can arise with certain bones, such as neurals 2 and 4, which typically share the same shape and lack a sulcus, making it challenging to ascertain whether two of these bones belong to a single individual or if they are from two individuals of different sizes. With these considerations in mind, we are confident in the identification of at least 21 individuals at various ontogenetic stages, including hatchlings, juveniles, and adults (Tab. 1).

Preparation of the specimens. One of the authors (B. Benítez) prepared the specimens using an air scribe. For the pieces of nearly complete shells, he used plaster to fill in the missing spaces. Finally, he attached metallic frameworks to some of the fossils for exhibition purposes. All the specimens are currently housed at the MAS, Socha, Boyacá Department, Colombia.

Strata dating. We collected two samples of sandstones near the Carbonera Creek UR-03 (3° 22' 12.71" N; 75° 8' 56.07" W) and UR-04 (3° 22' 12.21" N; 75° 8' 51.89" W), which make part of the *areniscas guía* following Velandia-Angarita *et al.* (2023) (Fig. 1.2–1.3). To extract zircon, we used crushing, magnetic separation, and heavy liquid techniques at Minerlab in Bogotá, Colombia. We dated zircon using U-Pb geochronology at the Department of Earth Science, UCSB. We mounted the zircons in epoxy mounts, polished to a 1 μm finish using diamond lapping film, imaged them under cathodoluminescence using a Quanta 400F field emission scanning electron microscope, and analyzed them using the LA-ICP-MS setup housed at the UCSB. Methods used in this study follow those outlined by Cottle *et al.* (2012, 2013) and Kylander-Clark *et al.* (2013).

To validate the results obtained by the LA-ICP-MS technique, we re-analyzed the zircons of UR-03 sample using the CA-ID-TIMS method (Mattinson, 2005). For a comprehensive and detailed procedure, see Online Supplementary Information. All errors are at 2.

Institutional acronyms. MAS, Museo de los Andes de Socha, Boyacá, Colombia; **UCSB,** University of California Santa Barbara, California, USA.

Other abbreviations. CA-ID-TIMS, chemical abrasion isotope dilution thermal ionization mass spectrometry; **LA-ICP-MS,** laser ablation inductively coupled plasma mass spectrometry; **MSWD,** mean squared weighted deviation; **PETM,** Paleocene–Eocene Thermal Maximum.

GEOLOGICAL SETTING

The Arcillolitas de Socha Formation is a sedimentary sequence composed of claystones, mudstones, sandstone layers, and some coal seams, measuring 370 m in thickness. It outcrops in the regions of Socha, Sochaviejo, and Paz del Río towns (Alvarado & Sarmiento, 1944; Ulloa & Rodríguez, 2003; Velandia-Angarita *et al.*, 2023). The lower to middle part of the formation has been dated as middle to late Paleocene (Van der Hammen, 1957; Jaramillo & Dilcher, 2001; Bayona *et al.*, 2020). The Arcillolitas de Socha Formation is interpreted as a result of sedimentation in lagoonal, marshy, paludal, and deltaic environments (Velandia-Angarita *et al.*, 2023).

Recently, Velandia-Angarita *et al.* (2023) described two fossiliferous horizons occurring in the upper member of the Arcillolitas de Socha Formation and briefly mentioned and figured the fossil content of them in five localities including La Cabrerita (Fig. 1.4), Carbonorte, and La Legua localities from the lower horizon, and El Reservorio (El Horizonte locality of Velandia-Angarita *et al.*, 2023) and Acopio Sur localities from the upper horizon (Fig. 1.2).

RESULTS

Strata dating. Seventy-one LA-ICP-MS analyses were obtained from detrital zircon from the rock sample UR-03, with the youngest five dates yielding a weighted mean age of 56.3±0.3 Ma (MSWD= 0.3). Six grains re-dated by CA-ID-TIMS yield a weighted mean of 56.83±0.04 Ma (MSWD= 1.2, probability of fit= 0.30). This is interpreted as the maximum depositional age. Other dates were 57.39±0.06, 57.39±0.14, and 57.24±0.06 Ma. Fifty LA-ICP-MS analyses were

obtained from detrital zircon from sample UR-04, with the youngest six dates yielding a weighted mean age of 57.2±0.5 Ma (MSWD= 1.4) (Online Supplementary Information). The LA-ICP-MS and CA-ID-TIMS dates indicate that the maximum depositional age for the *areniscas guía* between the two fossiliferous horizons is slightly older than the Paleocene–Eocene boundary and the warming event that characterized this interval, known as the PETM, which is dated to be 55.930 Ma (Westerhold *et al.*, 2017).

TABLE 1- List of selected specimens.

ID- number	Ontogenetic stage	Specimen	MLP	MWP
MAS-001	Adult	Partial carapace	1120	920
		Partial plastron	970	815
MAS-002	Adult	Nearly complete carapace	1020	800
		Nearly complete plastron	805	550
MAS-003	Adult	Partial carapace	1100	850
MAS-019	Adult	Left xiphiplastron	120	185
MAS-022	Juvenile	Nuchal bone	86	72
MAS-023	Juvenile	Right xiphiplastron	96	135
MAS-024	Juvenile	Right xiphiplastron	94	107
MAS-042	Juvenile	Left hypoplastron	116	140
MAS-050	Juvenile-adult	Right epiplastron	109	127
MAS-101	Adult	Peripheral bone	36	70
MAS-104	Juvenile-adult	Neurals 1 to 3, left costals 1 to 3	142	150
MAS-106	Juvenile	Right costal 1	131	210
MAS-107	Adult	Peripheral	103	137
MAS-108	Adult	Peripheral	121	143
MAS-152	Juvenile-adult	Entoplastron	88	101
MAS-1002	Juvenile	Left costal 1	114	188
MAS-1003	Juvenile	Left costal 1	131	220
MAS-Micro-199	Hatchling	Right hyoplastron	37	32
MAS-Micro-015	Hatchling	Nuchal	14	13
MAS-Micro-200	Hatchling	Left costal 1	20	29
MAS-Micro-296	Hatchling	Nuchal	19	20
MAS-Micro-086	Hatchling	Right costal 5	15	24

Corresponding to single individuals, their ontogenetic stage, and measurements as preserved. Abbreviations: **MLP,** maximum length as preserved; **MWP,** maximum width as preserved. Measurements in millimeters.

SYSTEMATIC PALEONTOLOGY

TESTUDINES Batsch, 1788
PLEURODIRA Cope, 1864
BOTHREMYDIDAE Baur, 1891
BOTHREMYDINI Gaffney *et al.*, 2006

Puentemys mushaisaensis Cadena *et al.*, 2012
Figure 2

Referred material. MAS-001 and MAS-002.
Localities and Age. The specimens come from La Cabrerita locality (6° 01' 59.69'' N; 72° 40' 06.52'' W), from the lower fossiliferous horizon. Considering the age that we obtained for the *areniscas guía* layers (see Results), stratigraphically located between the lower and upper fossiliferous horizons, La Cabrerita locality is late Paleocene in age.
Description. We describe first the most complete specimens and then the isolated bones as follow.

Specimen MAS-002 corresponds to an articulated shell (Fig. 2.1–2.4), with some missing portions of the carapace and plastron reconstructed with plaster, and a metallic framework attached to the fossil for display. Both the carapace and plastron are almost flat because of crushing and exhibit a smooth bone surface. The carapace misses the right peripherals 6 to 10, portions of the right peripherals 4 and 5, and most lateral regions of costals 3 to 8 (Fig. 2.1–2.2). The nuchal bone is slightly longer than wide exhibiting an erlenmeyer flask-like shape with straight posterolateral edges. The neural series is composed of six bones. Neural 1 is almost rectangular in shape and restricted between costals 1, the nuchal and neural 2. Neurals 2 to 5 are hexagonal in shape with shorter anterolateral margins and neural 4 is the largest and widest. The neural series ends with neural 6, which is pentagonal in shape, separating the anteromedial contact between costals 6. There are eight pairs of costals, of which, costals 6 to 8 contact each other medially. The suprapygal bone is pentagonal in shape, restricted between costals 8, the pygal and peripherals 11. There are 11 pairs of peripherals and a pygal bone, all of them being much wider than long.

The carapace of MAS-002 preserved well the sulci left by the scutes (Fig. 2.1–2.2). The cervical scute was absent.

There were 12 pairs of marginal scutes, square to rectangular in shape and restricted to the peripherals. Marginals 11 exhibited a particular pentagonal shape and were the only pair of marginals reaching the most lateral region of costals 8. There were five vertebral scutes, of which, vertebral 1 was the largest and widest, exhibiting an elongated hexagonal shape, and covering most of the posterior portions of the nuchal, peripherals 1, and a corner of peripherals 2, as well as most of neural 1 and the anteromedial portions of costals 1. Vertebral scutes 2 and 4 were narrower than vertebrals 1 and 5, and it seems it was the case for vertebral 3, for which the sulci are not well preserved. Vertebral 5 exhibited a particular shape with a posteromedial convex tip, and it covered entirely the suprapygal, most of costals 8, and the anterior portions of the pygal and peripherals 11. There were four pairs of pleural scutes, covering most of costals and reaching portions of peripherals.

The plastron of MAS-002 is almost completely preserved missing some lateral portions of the right hypoplastron and xiphiplastron, as well as a portion of the left mesoplastron (Fig. 2.3–2.4). The anterior plastral lobe is much shorter than the posterior one and exhibits a convex margin. Besides of being longer, the posterior plastral lobe is also a bit wider than the anterior one and exhibits a U-open shaped medial anal notch. The epiplastra are almost rectangular in shape meeting medially. The entoplastron is large, with anterolateral straight margins, convex posterior margins, and reaching almost the level of the carapace-plastron bridge. Both mesoplastra are large with convex medial edges. The hyoplastra and hypoplastra exhibit almost the same maximum length and are slightly longer than the xiphiplastral.

The sulci left by the plastral scutes are well-preserved in MAS-002 (Fig. 1.3–1.4), medially producing the following plastral formula: abdominals>femorals>anals>humerals> pectorals>gular. There was a pentagonal in shape gular scute that reached the most anterior corner of the entoplastron. Two extragular scutes were triangular and were restricted to the epiplastra. The humeral scutes met medially and covered most of the epiplastra, the entoplastron, and the anterior portions of the hyoplastra. The pectorals were shorter compared to the other scutes,

except to the gular and extragular scutes. The pectoro-abdominal sulci reached the anterior portion of both meso-plastra. The abdominal scutes were the largest of all the plastral scutes.

Specimen MAS-001 corresponds to an articulated shell (Fig. 2.5–2.6). Most of the bones of both the carapace and plastron are highly fractured in pieces, which using plaster we were able to assemble to their original anatomical position. However, it is not possible to clearly recognize the

sutures or sulci for most of both carapacial and plastral bones, except for some of the posterior peripherals of the carapace (Fig. 2.5). The anterior and most of the lateromedial portions of the carapace, as well as most of the anterior plastral lobe are missing, but reconstructed with plaster. The posterior plastral lobe exhibits convex lateral margins and a closed and deep U-shaped anal notch (Fig. 2.6).
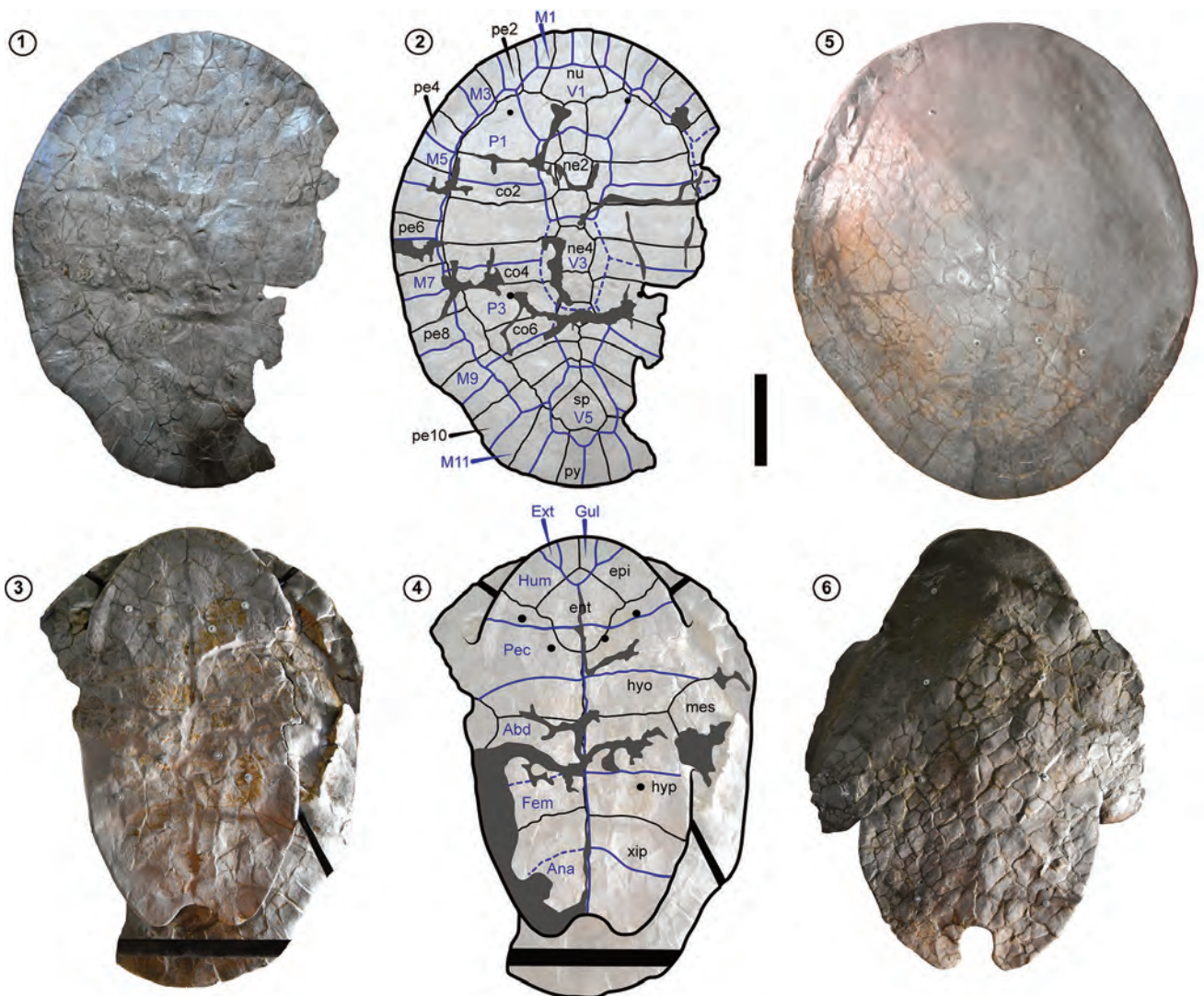

Figure 2. *Puentemys mushaisaensis* specimens from Arcillolitas de Socha Formation. **1−2, MAS-002** carapace in dorsal view; **3−4, MAS-002** plastron in ventral view; **5, MAS-001** carapace in dorsal view; **6, MAS-001** plastron in ventral view. Areas in gray indicate plaster filling. Black dots and lines indicate metalic framework. Blue lines indicate sulci. Abbreviations: **Abd,** abdominal scute; **Ana,** anal scute; **co,** costal bone; **ent,** entoplastron; **epi,** epiplastron; **Ext,** extragular scute; **Fem,** femoral scute; **Gul,** gular scute; **Hum,** humeral scute; **hyo,** hyoplastron; **hyp,** hypoplastron; **M,** marginal scute; **mes,** mesoplastron; **ne,** neural bone; **nu,** nuchal bone; **P,** pleural scute; **pe,** peripheral bone; **Pec,** pectoral; **py,** pygal scute; **sp,** suprapygal; **V,** vertebral scute; **xip,** xiphiplastron. Scale bar= 20 cm.

cf. *Puentemys mushaisaensis*
Figures 3–4

Referred material. MAS-019, MAS-022, MAS-023, MAS-024, MAS-042, MAS-050, MAS-101, MAS-104, MAS-107, MAS-108, MAS-120, MAS-152, MAS-1001, MAS-1002, MAS-1003, MAS-1004, MAS-1005, MAS-Micro-015, MAS-Micro-086, MAS-Micro-199, MAS-Micro-200, MAS-Micro-296.

Localities and Age. The fossil specimens conferred to *P. mushaisaensis* come from La Cabrerita locality (6° 01' 59.69'' N; 72° 40' 06.52'' W) from the lower fossiliferous horizon, from El Reservorio locality (El Horizonte locality of Velandia-Angarita *et al.*, 2023) (6° 01' 34.69'' N; 72° 39' 18.84'' W), and Acopio Sur locality (without name locality in Velandia-Angarita *et al.*, 2023) (6° 01' 27.05'' N; 72° 39' 15.41'' W) from the upper horizon (see Tab. 2). Considering the age that we obtained for the *areniscas guía* layers (see Results), stratigraphically located between the lower and upper fossiliferous horizons, La Cabrerita, La Legua, and Carbonorte localities are from the late Paleocene, and El Reservorio (El Horizonte) and Acopio Sur localities could correspond to the early Eocene.

Description. We describe first carapacial and plastral bones of large size individuals, representing juveniles and adults (Fig. 3), and then specimens representing hatchling individuals and some postcranial bones (Fig. 4). See Table 1 for the ontogenetic stage of most of the specimens and Table 2 for localities, year of collection, and measurements.

Specimen MAS-104 corresponds to a fragmentary carapace (Fig. 3.1–3.4), including the left costal 1, the medial portion of the left costal 2, a small portion of the left costal 3, and left lateral portions of neurals 1 to 3. On its dorsal surface (Fig. 3.1–3.2), the sulci left by vertebral scutes 1 and 2, and pleural 1 indicate that the vertebral scute 2 was wider anteriorly than posteriorly, and that the pleural 1 covered most of costal 1 and half of costal 2. In ventral view (Fig. 3.3–3.4), the axillary buttress scar is robust and projected laterally, almost parallel to the sutural contact between costals 1 and 2. Thus, the thoracic vertebrae 1 and 2 are also preserved and exhibit an elongated sand-clock shape.

Specimen MAS-1004 corresponds to a fragmentary carapace (Fig. 3.5–3.6), including the left costals 6 to 8 and portions of peripherals 9 to 11. In dorsal view, the sulci left by the pleural scute 4 and vertebral scute 4, as well as some of the marginal scutes are well-defined. Pleural scute was restricted to costals 6 to 8 and reached the medial portions of peripherals.

The specimens MAS-107 and MAS-108 correspond to two isolated peripheral bones (Fig. 3.7–3.10), potentially from the left posterior margin of the carapace, possibly peripherals 9 or 10 considering that their ventral surface is free of any scar, suggesting that they were part of the bridge region. On their dorsal surface, the sulci between marginal and pleural scutes are well-defined, indicating that the marginals were restricted to peripherals. Also, the bone surface of both peripherals exhibits some long groove shaped bioerosional scars. It is not possible to establish if they belonged to a single individual.

Specimen MAS-022 is a nuchal bone (Fig. 3.11–3.12). It has an almost pentagonal shape, being slightly longer than wide. In dorsal view, the sulci indicate that marginal scutes 1 contacted each other medially, which also means that the cervical scute was absent. The marginals 1 were very long, reaching the central portion of the nuchal, and a small notch at the anteromedial contact between marginals 1. The bone surface of the nuchal exhibits some long groove shaped bioerosional scars.

The specimens MAS-1002 and MAS-1003 correspond to two left costal 1 bones (Fig. 3.13–3.16). In ventral view of both bones, the axillary buttress scar reaches almost the posterior portion, near to the sutural contact with costal 2. Both axillary buttress scars exhibit the same shape, indicating that the bones belonged to the same taxon, representing two different individuals.

Specimen MAS-023 is a left xiphiplastron (Fig. 3.17–3.20). In ventral view, the sulcus between the femoral and anal scutes is well-defined. In visceral view, the pubis scar is almost oval in shape and the ischial scar is triangular and located close to the anal notch region. The anal notch exhibits a U-open shape and the most posterior end of the xiphiplastron forms a tip.

Specimen MAS-024 is a right xiphiplastron (Fig. 3.21–3.24). In visceral view, the pubis scar is almost oval in shape,
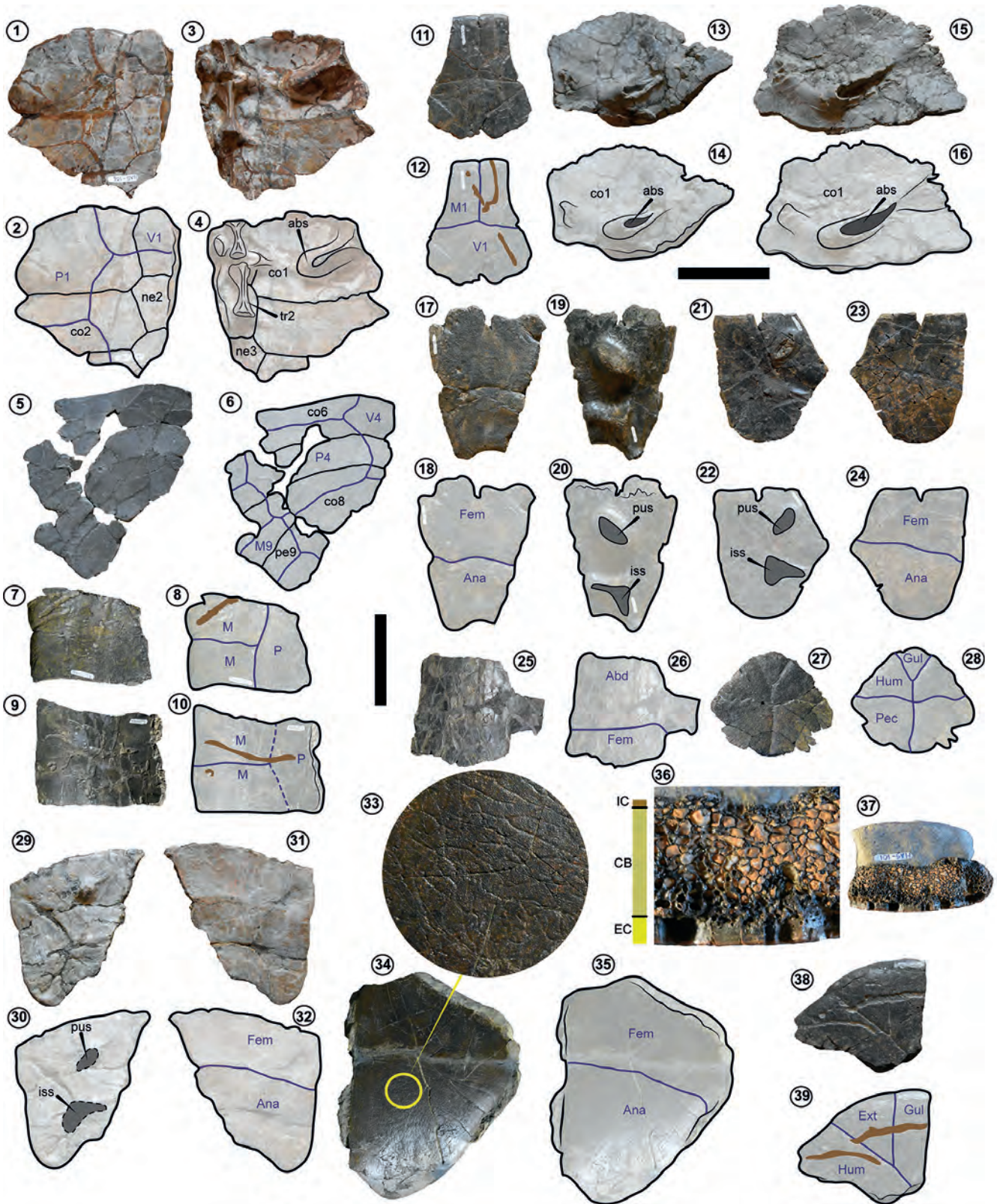
and the ischial scar is triangular and located anteriorly from the semicircular posterior end of the xiphiplastron. The anal notch exhibits a V-shape. In ventral view, the sulcus between the femoral and anal scutes is well-preserved.

Specimen MAS-042 corresponds to a left hypoplastron (Fig. 3.25–3.26). In ventral view, the sulcus between the abdominal and femoral scutes is visible ending laterally at the inguinal notch of the bone.

Specimen MAS-152 is an entoplastron (Fig. 3.27–3.28). It is diamond-shaped, preserving well the sulci between the humerals, the pectorals, and the gular scute. The gular scute was restricted to the anteromedial corner of the bone and the medial contact between the humeral was shorter than the contact between pectorals.

Specimen MAS-019 corresponds to a left xiphiplastron (Fig. 3.29–3.32). In visceral view, the pubis scar is almost oval in shape and the ischial scar is triangular and located anteriorly from the semicircular posterior end of the xiphiplastron. The anal notch exhibits a V-open shape. In ventral view, the sulcus between the femoral and anal scutes is well-preserved.

Specimen MAS-120 corresponds to a nearly complete left xiphiplastron (Fig. 3.33–3.35). In ventral view, the sulcus between the femoral and anal scutes is well-preserved and located relatively anteriorly to the posterior tip of the bone. The bone surface exhibits a distinct dichotomic sculptural pattern (Fig. 3.33).

Specimen MAS-101 is a plastral bone fragment (Fig. 3.36–3.37). It might correspond to a lateral fragment of a right hypoplastron. In cross-section of the bone (Fig. 3.36), the three tissue layers of bone are recognizable (inner, cancellous and external). The inner cortex is the thinnest of the three layers and the external cortex exhibits parallel lines of different colors. The cancellous (spongy) tissue forms a trabecular pattern, with the cavities increasing in size towards the ventral region of the bone.

Specimen MAS-050 is a partial right epiplastron (Fig. 3.38–3.39). In ventral view, the sulci show that the extragular scute was triangular in shape and restricted to the epiplastron, without reaching the entoplastron. The bone surface exhibits some long groove shaped bioerosional scars.

The specimens MAS-Micro-015 and MAS-Micro-296 correspond to two small nuchal bones (Fig. 4.1–4.4). Both exhibit an almost pentagonal shape, being slightly longer than wide. In dorsal view, the sulci indicate that marginal scutes 1 contacted each other medially, which also means that the cervical scute was absent. The marginals 1 covered the nuchal until half of its length. In the case of MAS-Micro-296 specimen, the bone surface exhibits some small circular to elongated bioerosional scars.

Specimen MAS-Micro-200 is a left costal 1 (Fig. 4.5–4.8). In dorsal view, the sulci between vertebrals 1 and 2 and pleural 1 scutes are visible. In ventral view, the axillary buttress scar occupies most of the mid-lateral portion of the bone. The medial edge of the bone indicates that neural 1 was a very elongated bone.

Specimen MAS-Micro-086 corresponds to a right costal 5 (Fig. 4.9–4.12). It has a wider lateral region, and it is attributed as right costal 5 because it has the inguinal buttress scar at its lateral margin, as it is common in other bothremydids and in general in pelomedusoids. In dorsal view, the sulci between vertebrals and pleural scutes are visible indicating a relatively narrow vertebral scutes.

Figure 3. cf. *Puentemys mushaisaensis* specimens from Arcillolitas de Socha Formation, juvenile and adults. **1–2, MAS-104** fragmentary carapace in dorsal view; **3–4, MAS-104** fragmentary carapace in ventral view; **5–6, MAS-1004** fragmentary left posterior side of a carapace; **7–8, MAS-107** isolated peripheral in dorsal view; **9–10, MAS-108** isolated peripheral in dorsal view; **11–12, MAS-022** nuchal bone in dorsal view; **13–14, MAS-1002** left costal 1 in ventral view; **15–16, MAS-1003** left costal 1 in ventral view; **17–18, MAS-023** a left xiphiplastron in ventral view; **19–20, MAS-023** a left xiphiplastron in visceral view; **21–22, MAS-024** a right xiphiplastron in visceral view; **23–24, MAS-024** a right xiphiplastron in ventral view; **25–26, MAS-042**, a left hypoplastron in ventral view; **27–28, MAS-152**, an entoplastron in ventral view; **29–30, MAS-019**, left xiphiplastron in visceral view; **31–32, MAS-019**, left xiphiplastron in ventral view; **33–35, MAS-120**, a nearly complete left xiphiplastron in ventral view, and zoom-up of the bone surface showing dichotomic sculpturing pattern; **36–37, MAS-101**, a plastral bone fragment in cross section showing the three tissue layers (internal cortex, cancellous bone, and external cortex); **38–39, MAS-050**, a partial right epiplastron in ventral view. Brown regions indicate long groove shaped bioerosional scars. Blue lines indicate sulci. Gray regions indicate scars. Abbreviations: **Abd,** abdominal scute; **abs,** axillary buttress scar; **Ana,** anal scute; **CB,** cancellous bone; **co,** costal bone; **EC,** external cortex; **Ext,** extragular scute; **Fem,** femoral scute; **Gul,** gular scute; **Hum,** humeral scute; **IC,** internal cortex; **iss,** ischial scar; **M,** marginal scute; **ne,** neural bone; **nu,** nuchal bone; **P,** pleural scute; **pe,** peripheral bone; **Pec,** pectoral scute; **pus,** pubis scar; **tr,** thoracic vertebra; **V,** vertebral scute. Vertical scale bar (= 10 cm) applies for 1 to 10 and 29 to 32. Horizontal scale bar (= 5 cm) applies for 11 to 28 and 33 to 39.

TABLE 2- Full list of specimens referred in this study.

ID- number	Locality	Year of collection	Figure
MAS-001	La Cabrerita	2012	2.5−2.6
MAS-002	La Cabrerita	2012	2.1−2.4
MAS-019	Acopio Sur	2011	3.29−3.32
MAS-022	El Reservorio	2010	3.11−3.12
MAS-023	El Reservorio	2010	3.17−3.20
MAS-024	El Reservorio	2010	3.21−3.24
MAS-042	El Reservorio	2010	3.25−3.26
MAS-050	El Reservorio	2005	3.38−3.39
MAS-101	La Cabrerita	2010	3.36−3.37
MAS-104	Acopio Sur	2010	3.1−3.4
MAS-107	El Reservorio	2005	3.7−3.8
MAS-108	El Reservorio	2005	3.9−3.10
MAS-120	La Cabrerita	2015	3.33−3.35
MAS-152	El Reservorio	2008	3.27−3.28
MAS-1005	Acopio Sur	2010	4.15−4.16
MAS-1001	Acopio Sur	2010	4.17
MAS-1002	Acopio Sur	2010	3.13−3.14
MAS-1003	Acopio Sur	2010	3.15−3.16
MAS-1004	Acopio Sur	2010	3.5−3.6
MAS-Micro-199	El Reservorio	2008	4.13−4.14
MAS-Micro 015	El Reservorio	2008	4.1−4.2
MAS-Micro 200	El Reservorio	2008	4.5−4.8
MAS-Micro 296	El Reservorio	2008	4.3−4.4
MAS-Micro 086	El Reservorio	2008	4.9−4.12

Specimen MAS-Micro-199 is a right hyoplastron (Fig. 4.13−4.14). In ventral view, the sulci left by the plastral scutes are preserved indicating that the pectorals had a long medial contact, and that the pectoro-abdominal sulcus ends laterally without reaching the mesoplastron.

Specimen MAS-1005 is a right pubis bone (Fig. 4.15−4.16). In medial view has a boomerang-like shape, showing a short epipubis that faces ventrally. The lateral process of the pubis ends in a rugose nearly oval surface for the articulation with the xiphiplastron.

Specimen MAS-1001 is a right scapula (Fig. 4.17). The bone suffered some degree of deformation and fracturing, particularly at its acromial process. The glenoid fossa is relatively well preserved. However, due to the preservation it is not possible to estimate the original internal angle formed by the two processes that form the scapula.

DISCUSSION
Taxonomic affinity

The shells MAS-001 and MAS-002 share the following features with *Puentemys mushaisaensis* and other members of the Bothremydini tribe: 1) a carapace highly circular in
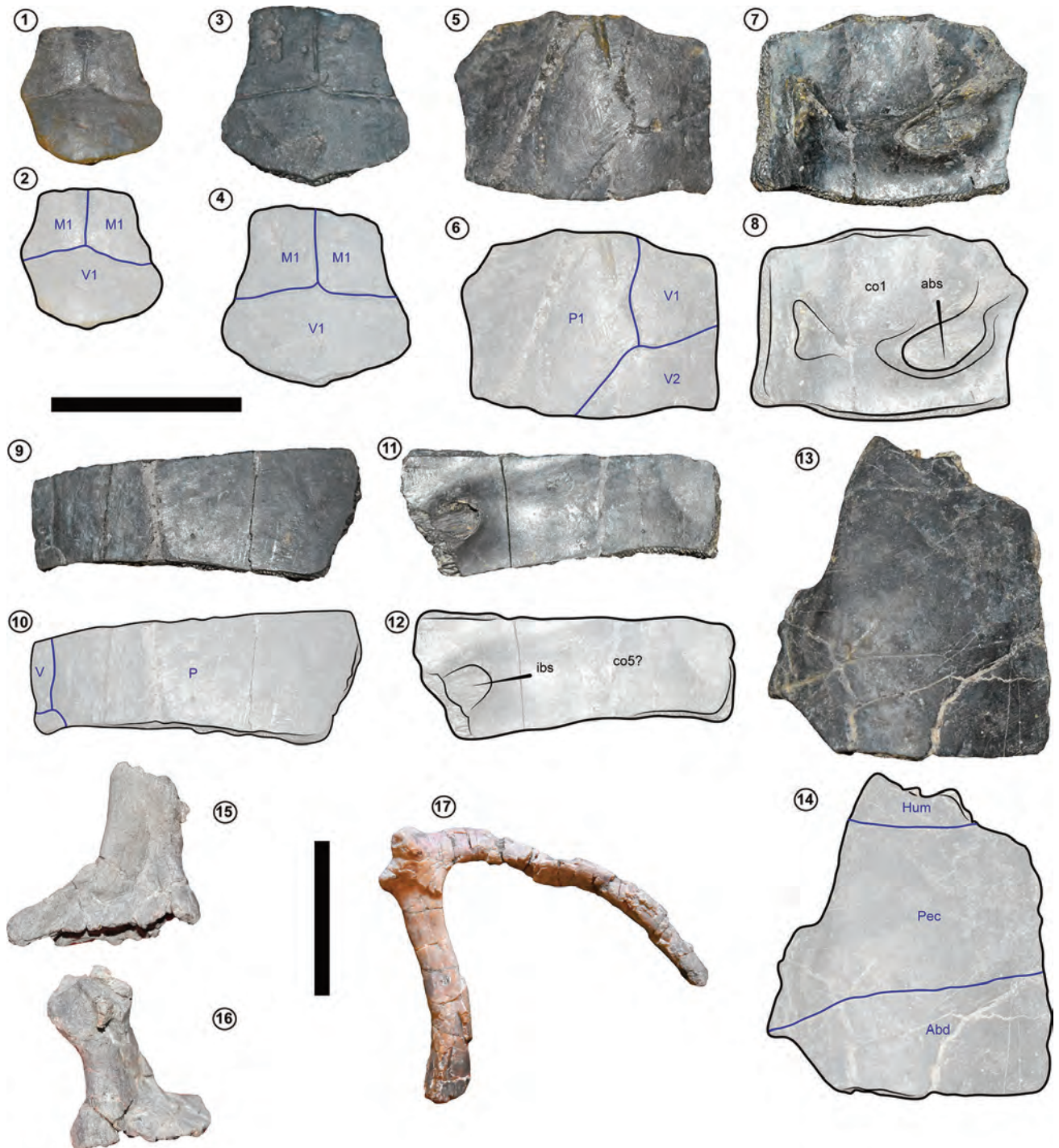
Figure 4. cf. *Puentemys mushaisaensis* specimens from Arcillolitas de Socha Formation hatchling individuals and some postcranial bones. **1–2, MAS-Micro-015**, small nuchal bone in dorsal view; **3–4, MAS- Micro-296**, small nuchal bone in dorsal view; **5–6, MAS-Micro-200**, a left costal 1 in dorsal view; **7–8, MAS-Micro-200**, a left costal 1 in ventral view; **9–10, MAS-Micro-086**, a right costal 5 in dorsal view; **11–12, MAS-Micro-086**, a right costal 5 in ventral view; **13–14, MAS-Micro-199**, a right hyoplastron in ventral view; **15–16, MAS-1005**, a right pubis bone in medial and anterior views respectively; **17, MAS-1001**, a right scapula in dorsal view. Blue lines indicate sulci. Abbreviations: **Abd,** abdominal scute; **abs,** axillary buttress scar; **co,** costal bone; **Hum,** humeral scute; **ibs,** inguinal buttress scar; **M,** marginal scute; **Pec,** pectoral scute; **P,** pleural scute; **V,** vertebral scute. Horizontal scale bar (= 2 cm) applies for 1 to 14. Vertical scale bar (= 5 cm) applies for 15 to 17.

159

outline; 2) marginal scutes restricted to the peripherals; 3) a shorter and narrower anterior plastral lobe in contrast to the posterior one; 4) large entoplastron reaching the level of the axillary notch or carapace-plastron bridge. Specifically, MAS-002 specimen shares with *P. mushaisaensis* the following additional features: 1) a vertebral scute 1 much wider than the others and reaching the peripherals 2; and 2) pectoral scutes shorter than humerals, abdominals, and femorals. Some differences exist between MAS-002 specimen and specimens of *P. mushaisaensis* from the Cerrejón Formation, including: 1) six neurals, instead of seven as in the specimens from Cerrejón Formation, condition that allows the medial contact between costals 6 in MAS-002; and 2) marginals 11 exhibiting pentagonal shape and reaching a small portion of costals 8. We consider these two anatomical differences between the Cerrejón and Socha specimens as potentially explained by intraspecific variability inside *P. mushaisaensis*, and considering that so far, we only have found a single nearly complete and well-preserved specimen (MAS-002), we avoid erecting a new taxon for *Puentemys*.

For the case of the partial and isolated bones of Figures 3 and 4, their taxonomic affinity is more difficult to establish. However, some of them share features with specimens of *P. mushaisaensis*, those described in Cadena *et al.* (2012) and this study. For instance, the anteromedial notch between marginals 1 of the nuchal bone in MAS-022 specimen, the dichotomic sculpturing pattern exhibited by the left xiphiplastron in MAS-120 specimen, and the bone tissue pattern shown by MAS-101 specimen (Fig 3.36). Based on these similarities, and in absence of more complete specimens, we include all these fossils under cf. *Puentemys mushaisaensis*, hoping that future fieldworks and findings can validate or reject this hypothesis which is plausible, considering that the fragmentary material (cf. *P. mushaisaensis*) has been found in the same horizons as indisputable specimens of *P. mushaisaensis*.

Paleobiogeographical implications

Bohtremydid turtles were particularly diverse and widespread during the Cretaceous (Gaffney *et al.*, 2006; Pérez-García *et al.*, 2017; Pérez-García, 2018b, 2020; Paleobiology Database November, 2023, and references therein; Fig. 5.1).

At the beginning of the Cenozoic, particularly during the Paleocene, they still ocurred in almost all continents, except Oceania and Antarctica (Paleobiology Database November, 2023; Fig. 5.2), and during the Eocene (Paleobiology Database November, 2023; Fig. 5.3) they started to decrease in occurrence and geographical distribution, becoming mostly restricted to mid to lower latitudes. The occurrence of *P. mushaisaensis* and cf. *P. mushaisaensis* from the Arcillolitas de Socha Formation describe herein, *P. mushaisaensis* from the Cerrejón Formation (Cadena *et al.*, 2012), and *Motelomama olssoni* from Perú (Pérez-García *et al.*, 2018a), indicate that bothremydid turtles inhabited northern South America from at least the middle to late Paleocene until the early Eocene, surviving both the PETM and the Early Eocene Climatic Optimum (Fig. 5.2–5.3).

The paleofauna of the Arcillolitas de Socha Formation also exhibits identical taxonomic affinities with the middle to late Paleocene fauna from the Cerrejón Formation, including the occurrence of *P. mushaisaensis*, as well as crocodiles and snakes mentioned in Velandia-Angarita *et al.* (2023), which are currently under study. The similarity between both paleofaunas allows us to formulate the following paleobiogeographical considerations. First, taking into account the palinspastic paleogeographic reconstruction of northern South America during the Paleogene (Bayona, 2018), it is evident that there was a connectivity between northern deltaic and coastal environments where sediments of the Cerrejón Formation were accumulated, with the fluvial deposits of the Arcillolitas de Socha and Bogotá formations (Fig. 5.4–5.5). This implies that favorable ecosystems for the development of a giant herpetofauna occurred from north to south, forming a faunistic corridor of at least 300 km in length during the middle Paleocene to at least the early Eocene (Fig. 5.4).

A more extensive habitat was crucial not only for the migration of the fauna, including the bothremydid turtles, but could also have played a key role other than a warmer climate in maintaining their large size (Vermeij, 2016; Ferrón *et al.*, 2017; Maher *et al.*, 2022, and references therein), similar to what happened during the Miocene in northern South America with the Pebas System (Scheyer *et al.*, 2013, Cadena *et al.*, 2020, and references therein). Whether the Paleocene–Eocene faunistic corridor persisted until the
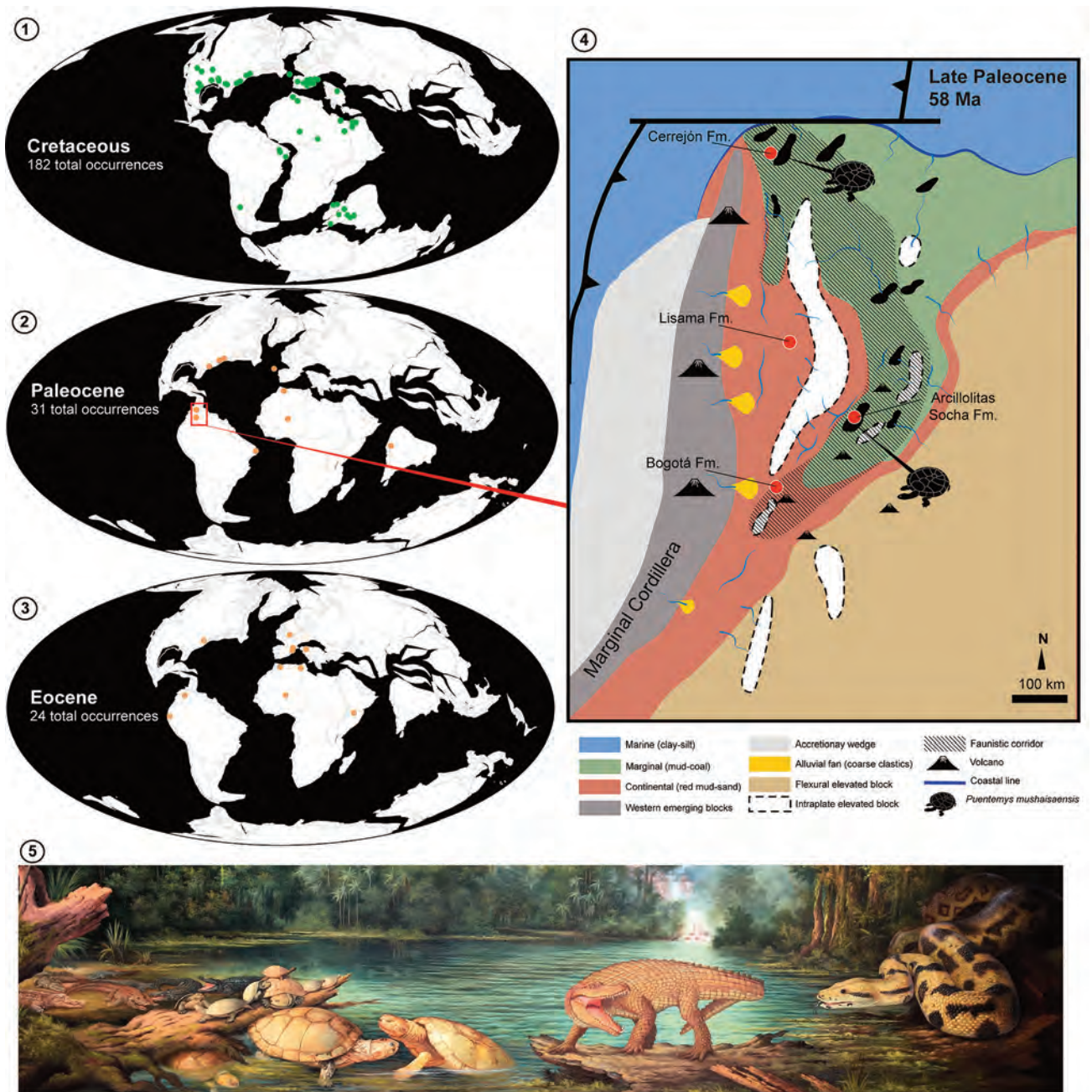
Figure 5. Paleobiogeographic distribution of bothremydids including *Puentemys mushaisaensis* and artistic reconstruction of Socha paleofauna. **1,** Fossil record of Cretaceous bothremydids plotted at 105 Ma from Paleobiology Database (2023); **2,** fossil record of Paleocene bothremydids plotted at 61 Ma from Paleobiology Database (2023), **3,** fossil record of Eocene bothremydids plotted at 44 Ma from Paleobiology Database (2023); **4,** palinspastic paleogeographic reconstruction of northern South America for the Paleocene–Eocene, modified from Bayona (2018), including the occurrences of *Puentemys mushaisaensis* from Cerrejón and Socha regions; **5,** artistic reconstruction of the Socha paleofauna and ecosystem by B. Benítez.

late Eocene or the Oligocene, and if the bothremydid turtles and other vertebrates kept inhabiting northern South American environments during those epochs, is still unknown.

CONCLUSIONS

The fossil record of northern South America is increasing rapidly as we show in this study, with the first fully description of the bothremydid turtles, particularly of

Puentemys mushaisaensis from the late Paleocene and early Eocene Arcillolitas de Socha Formation. This discovery expands further south the biogeographical occurrence of *P. mushaisaensis*, now known from both the Cerrejón Coal Mine and the Socha regions, which were separated by at least 500 km. Thus, the identical composition of both paleofaunas (Cerrejón and Socha), including *P. mushaisaensis* and other vertebrates currently under study, supports the existence, during the late Paleocene to early Eocene, of a larger ecosystem with connectivity between coastal and more inland continental regions in northern South America. This created a faunistic corridor that not only facilitated migration of these vertebrates but also, together with warmer conditions, supported the development of a large-sized herpetofauna. A challenge still exists for neotropical vertebrate paleontology, which is to find late Eocene and Oligocene fossil vertebrates that will allow to improve our understanding of the evolution of neotropical faunas.

ACKNOWLEDGMENTS

REFERENCES

Alvarado, B. & Sarmiento, R. (1944). *Informe geológico general sobre los yacimientos de hierro, carbón y caliza de la región de Paz de Río, departamento de Boyacá*. [Servicio Geológico Nacional Unpublished Report].

Bayona, G. (2018). The onset of the mountain uplift in the northern Andes: A perspective based on Coniacian to Paleocene tectono-sedimentary studies. *Revista de la Academia Colombiana de Ciencias Exactas Físicas y Naturales*, *42*(165), 364–378.

Bayona, G., Baquero, M., Ramírez, C., Tabares, M., Salazar, A. F., Nova, G., Duarte, E., Pardo, A., Plata, A., Jaramillo, C., Rodríguez, G., Caballero, V., Cardona, A., Montes, C., Gómez-Marulanda, S., & Cárdenas-Rozo, A. (2020). Unraveling the widening of the earliest Andean northern orogen: Maastrichtian to early Eocene intra-basinal deformation in the northern Eastern Cordillera of Colombia. *Basin Research*, *33*(1), 809–845. https://doi.org/10.1111/bre.12496

Cadena, E. A., Bloch, J. I., & Jaramillo, C. A. (2012). New bothremydid turtle (Testudines, Pleurodira) from the Paleocene of northeastern Colombia. *Journal of Paleontology*, *86*(4), 688–698. https://doi.org/10.1666/11-128R1.1

Cadena, E. A., Scheyer, T. M., Carrillo-Briceño, J. D., Sánchez, R., Aguilera-Socorro, O. A., Vanegas, A., Pardo, M., Hansen, D. M., & Sánchez-Villagra, M. R. (2020). The anatomy, paleobiology, and evolutionary relationships of the largest extinct side-necked turtle. *Science Advances*, *6*(7), eaay4593.

https://doi.org/10.1126/sciadv.aay4593

Cottle, J. M., Burrows, A. J., Kylander-Clark, A. R. C., Freedman, P. A., & Cohen, R. (2013). Enhanced sensitivity in laser ablation multi-collector inductively coupled plasma mass spectrometry. *Journal of Analytical Atomic Spectrometry*, *28*(11), 1700–1706.

Cottle, J. M., Kylander-Clark, A. R. C., & Vrijmoed, J. C. (2012). U-Th/Pb geochronology of detrital zircon and monazite by Single Shot Laser Ablation Inductively Coupled Plasma Mass Spectrometry (SS-LA-ICPMS). *Chemical Geology*, *332–333*, 136–147. https://doi.org/10.1016/j.chemgeo.2012.09.035

De Araújo-Carvalho, A. R., Ghilardi, A. M., & Franca-Barreto, A. M. (2016). A new side-neck turtle (Pelomedusoides: Bothremydidae) from the Early Paleocene (Danian) Maria Farinha Formation, Paraíba Basin, Brazil. *Zootaxa*, *4126*(4), 491–513. http://doi.org/10.11646/zootaxa.4126.4.3

Ferrón, H. G., Martínez-Pérez, C., & Botella, H. (2017). The evolution of gigantism in active marine predators. *Historical Biology*, *30*(5), 712–716. https://doi.org/10.1080/08912963.2017.1319829

Gaffney, E. S., Tong, H., & Meylan, P. A. (2006). Evolution of the side-necked turtles: the families Bothremydidae, Euraxemydidae, and Araripemydidae. *Bulletin of the American Museum of Natural History*, *300*, 1–698. https://doi.org/dgxpvn

Jaramillo, C. A. & Dilcher, D. L. (2001). Middle Paleogene palynology of central Colombia, South America: A study of pollen and spores from tropical latitudes. *Palaeontographica Abteilung B*, *258*, 87–213.

Kylander-Clark, A. R. C., Hacker, B. R., & Cottle, J. M. (2013). Laser-ablation split-stream ICP petrochronology. *Chemical Geology*, *345*, 99–112. https://doi.org/10.1016/j.chemgeo.2013.02.019

Lapparent de Broin, F. de. (2000). African chelonians from the Jurassic to the present. A preliminary catalog of the African fossil chelonians. *Palaeontologia Africana*, *36*, 43–82.

Lapparent de Broin, F. de., Métais, G., Bartolini, A., Brohi, I. A., Lashari, R. A., Marivaux, L., Merle, D., Warar, M. A., & Solangi, S. H. (2021). First report of a bothremydid turtle, *Sindhochelys ragei* n. gen., n. sp., from the early Paleocene of Pakistan, systematic and palaeobiogeographic implications. *Geodiversitas*, *43*(25), 1341–1363.

https://doi.org/10.5252/geodiversitas2021v43a25.

Maher, A. E., Burin, G., Cox, P. G., Maddox, T. W., Maidment, S. C. R., Cooper, N., Schachner, E., & Bate, K. T. (2022). Body size, shape and ecology in tetrapods. *Nature Communications*, *13*(1), 4340. https://doi.org/10.1038/s41467-022-32028-2

Mattinson, J. M. (2005). Zircon U-Pb chemical abrasion ("CA-TIMS") method: combined annealing and multi-step partial dissolution analysis for improved precision and accuracy of zircon ages. *Chemical Geology*, *220*(1-2), 47–66.
https://doi.org/10.1016/j.chemgeo.2005.03.011

Paleobiology Database. (2023). *Paleobiogeographic distribution of bothremydids*. Retrieved November 15th 2023 from https://paleobiodb.org/#/

Pérez-García, A. (2016). A new turtle taxon (Podocnemidoidea, Bothremydidae) reveals the oldest known dispersal event of the crown Pleurodira from Gondwana to Laurasia. *Journal of Systematic Palaeontology*, *15*(9), 1–23. https://doi.org/10.1080/14772019.2016.1228549

Pérez-García, A. (2018a). New genera of Taphrosphyina (Pleurodira, Bothremydidae) for the French Maastrichtian '*Tretosternum*' *ambiguum* and the Peruvian Ypresian '*Podocnemis*' *olssoni*. *Historical Biology*, *32*(4), 555–560.
https://doi.org/10.1080/08912963.2018.1506779

Pérez-García, A. (2018b). New information on the Cenomanian bothremydid turtle *Algorachelus* based on new, well-preserved

material from Spain. *Fossil Record*, *21*(1), 119−135. https://doi.org/10.5194/fr-21-119-2018

Pérez-García, A. (2020). First evidence of a bothremydid turtle (crown Pleurodira) in the middle Cretaceous of Castile and Leon (Spain). *Journal of Iberian Geology*, *46*, 363−368. https://doi.org/10.1007/s41513-020-00146-9

Pérez-García, A., Antunes, M. T., Barroso-Barcenilla, F., Callapez, P. M., Segura, M., Soares, A. F., & Torices, A. (2017). A bothremydid from the middle Cenomanian of Portugal identified as one of the oldest pleurodiran turtles in Laurasia. *Cretaceous Research*, *78*, 61−70. https://doi.org/10.1016/j.cretres.2017.05.031

Scheyer, T. M., Aguilera, O. A., Delfino, M., Fortier, D. C., Carlini, A. A., Sánchez, R., Carrillo-Briceño, J. D., Quiroz, L., & Sánchez-Villagra, M. R. (2013). Crocodylian diversity peak and extinction in the late Cenozoic of the northern Neotropics. *Nature Communications*, *4*(1), 1907. https://doi.org/10.1038/ncomms2940

Schmidt, K. P. (1931). A fossil turtle from Peru. *Field Museum of Natural History, Geological Series*, *4*, 251−254.

Ulloa, C. & Rodríguez, E. (2003). *Memoria de la plancha 172 Paz de Río, Bogotá, Colombia, INGEOMINAS*. Retrieved from https://recordcenter.sgc.gov.co/B4/13010010024481/documento/pdf/0101244811101000.pdf

Van Der Hammen, T. (1957). *Estratigrafía palinológica de la sabana de Bogotá, cordillera oriental de Colombia*. [Instituto Geológico Nacional Unpublished Report].

Velandia-Angarita, O. R., Mariño-Martínez, J. E., & Giraud-López, M. J. (2023). Litoestratigrafía y bioestratigrafía como herramientas de exploración de fósiles de vertebrados en Socha (Colombia). *Revista EIA*, *20*(40), 1−20. https://doi.org/10.24050/reia.v20i40.1700

Vermeij, G. J. (2016). Gigantism and its implications for the history of life. *PLOS ONE*, *11*, e0146092.

Westerhold, T., Röhl, U., Frederichs, T., Agnini, C., Raffi, I., Zachos, J. C., & Wilkens, R. H. (2017). Astronomical calibration of the Ypresian timescale: implications for seafloor spreading rates and the chaotic behavior of the solar system? *Climate of the Past*, *13*(9), 1129−1152. https://doi.org/10.5194/cp-13-1129-2017